Low Temperature Physics/Fizika Nizkikh Temperatur, 2021, vol. 47, No. 6, pp. 491–500

Effect of compression in molecular spin-crossover chains

A. Gudyma

Max Planck Institute of Microstructure Physics, Weinberg 2, 06120 Halle/Saale, Germany

Iu. Gudyma

Physical Technical and Computer Sciences Institute of Yuriy Fedkovych Chernivtsi National University Chernivtsi 58012, Ukraine

E-mail: yugudyma@gmail.com

Received March 11, 2021, published online April 26, 2021

The thermodynamic properties of a one-dimensional spin-crossover molecular chain under constant external pressure are investigated. The effective compressible degenerate Ising model is used as a theoretical basis. Analytical results for the crossover from low to high spin are obtained using the transfer matrix formalism. Exact expressions are obtained for the fraction of molecules in the high-spin state, the correlation function, and the heat capacity. The analysis of the range of parameters in which the spin-crossover occurs is carried out, and it is shown how the pressure changes the position of the crossover.

Keywords: spin-crossover, molecular chain, Ising model, magnetization, phonons.

1. Introduction

The research of bistable molecular systems is a challenging field of modern scientific study. The magnetic spin transition associated with the spin-crossover (SCO) phenomenon represents a paradigm of bistability at the molecular level that is of current interest because of potential applications in the development of new generations of electronic devices such as nonvolatile memories, molecular sensors, and displays [1–3]. The interconversion of two spin states is observed in iron(II) coordination compounds in octahedral surroundings. In these ones the paramagnetic high spin state (HS, $S = 2$) can be switched reversibly to the low spin state (LS, $S = 0$) by several external stimuli such as temperature, pressure or light irradiation, yielding significant structural, magnetic, and optical changes [3–7]. In general, the spin-crossover materials are the class of inorganic coordination complexes of the chemical elements with $3d^4$–$3d^7$ electronic configuration of the outer orbital which form the ligand environment with the first-row transition metal ion centered in octahedral ligand field. These complexes can be reversibly switched between spin states, resulting in different magnetic, structural or optical properties.

The microscopic Ising-like model can be used for describing the behavior of spin-crossover crystals at molecular level. Different energies and degeneracies of the HS and LS states can be taken into account as an effective temperature dependent field. Low dimensional iron(II) spin transitional materials were a subject of recent experimental studies in both one-dimensional (1D) [8–13] and two-dimensional (2D) [14–16] with various techniques and setups. Note that the finite-size effects are important for the understanding of the practical application of the real low-dimensional system. In one dimension such materials may be described by Ising-like models and many important results obtained analytically [17–22]. The one-dimensional Ising-like model plays an important role in statistical physics, being one of the models which have been solved exactly. Compressible Ising model also has along history of study [23–25], and new results were obtained recently by numeric techniques [26–31]. Real quasi-1D spin-crossover materials almost perfectly correspond to the one-dimensional Ising model causing particular interest for theoretical studies.

Elastic degrees of freedom cause change of the thermodynamic properties of the system. It is known that the free HS ferrous ion has a larger volume than the LS one. Due to the difference in the effective volume of HS and LS chains of spin crossover materials are sensitive to external pressure [32]. Therefore, the pressure becomes an important parameter for describing the system. For example, the influence of pressure has been used to tune the spin transition properties of such 1D chain compounds. In previous papers [33–35] by one of the authors, the deformations were considered as homogeneous and isotropic. Such a compressible model is the simplest special case of consideration

of the elastic nature of molecular crystals. In this work we study effects of the constant external pressure on the thermodynamics properties of the spin crossover materials.

The outline of this work is as follows. Section 2 defines the model's formalism. In Sec. 3 we calculate the partition function and introduce effective Ising-like Hamiltonian with temperature dependent ferromagnetic constant and magnetic field. Given model is solved analytically using transfer matrix formalism, which we introduce in the Sec. 4. We demonstrate on the example of the system's volume and the correlation function how to make exact finite N calculations in Sec. 5. The specific heat capacity and susceptibility are obtained in Sec. 6. In the remaining Sec. 7 part of the manuscript, we focus on analytical and numerical results for spin-crossover molecular chain under the pressure. Finally, results and discussions are given in Sec. 8.

2. Model

In this work, we study behavior of a molecular chain under the external pressure. Each particle in the chain occurs in one of two states which have different properties, and may freely switch from one state to another. We denote these states as the high spin pseudo-state and low spin pseudo-state. We introduce single-particle quasi-spin operator $\hat{s}$ as an operator which has eigenvalue +1 for the HS state and eigenvalue –1 for the LS state. Let's denote the degeneracy of the pseudo-spin states s_n as g_{s_n}, where $g_{s_n} = g_+$ for spin $s_n = +1$ pseudo-state and $g_{s_n} = g_-$ for $s_n = -1$ pseudo-state. We assume pair interactions of the molecules in the LS–LS, LS–HS and HS–HS pairs are different and we denote the corresponding pair potentials as $V_{--}(r)$, $V_{+-}(r)$, and $V_{++}(r)$. In Fig. 1(a) we schematically illustrate all possible pseudo-spin configurations of the pairs of molecules. In similar models, like for example in the two-variable anharmonic Ising-like model [18, 36] V_{--}, V_{+-}, and V_{++} potentials are often referred as the LS, HL, and HS elastic potentials. Specific parameters of the interaction potentials can be extracted from experimental measurements, like x-ray diffraction [37] or Brillouin spectroscopy [38].

The Hamiltonian of system consists of the Hamiltonian of the molecular chain and term describing action of the external pressure

$$\hat{H} = \hat{H}_{MC} + \hat{H}_P. \tag{1}$$

The molecular chain Hamiltonian is a sum of the pair potentials and single particle field

$$\hat{H}_{MC} = \sum_{n=1}^{N-1} V_{s_n s_{n+1}}(x_n - x_{n+1}) + \sum_{n=1}^{N} W_{s_n}, \tag{2}$$

where N is the total number of molecules in the chain and W_{s_n} is the energy of the single-molecule pseudo-state. The difference of the pseudo-state energies $\Delta = W_+ - W_-$ is the external ligand field acting on a single molecule. Action of the external pressure P is described by the following extra term in the Hamiltonian

$$\hat{H}_p = PL, \tag{3}$$

where $L = x_N - x_1$ is the effective volume of the one-dimensional system. We apply a harmonic approximation for the nearest-neighbor pair potential $V_{s_n s_{n+1}}(r)$ at the potential minimum

$$V_{s_n s_{n+1}}(r) = V^{(0)}_{s_n s_{n+1}} + \frac{1}{2} K_{s_n s_{n+1}} \left(r - a_{s_n s_{n+1}} \right)^2, \tag{4}$$

where $a_{s_n s_{n+1}}$ is the average distance between the particles at the equilibrium, $V^{(0)}_{s_n s_{n+1}} = V_{s_n s_{n+1}}(a_{s_n s_{n+1}})$ is the potential

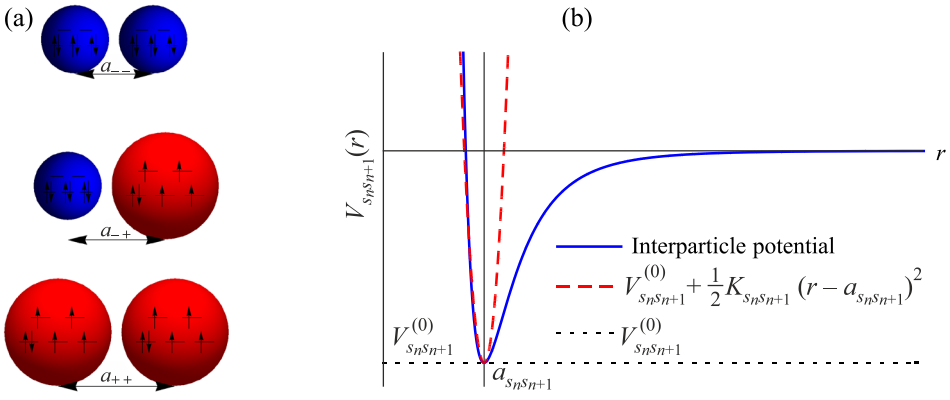

Fig. 1. (Color online) Schematic interactions of the pseudo-spin states and treatment of the inter-particle potential. (a) All possible configurations of the nearest pseudo-spin states. Molecules in the LS and HS state are illustrated with blue and red, correspondingly. Interaction potentials and average distances between particles depend on the pseudo-spin states. (b) Interaction potential and harmonic approximation. We consider possible displacement of the particles from the equilibrium position for the given pseudo-state configuration to be small.

depth and $K_{s_n s_{n+1}}$ is an elastic constant coupling nth and $(n+1)$st molecules in the pseudo-states s_n and s_{n+1} respectively. In Fig. 1(b) we illustrated treatment of the $V_{--}(r)$, $V_{+-}(r)$ and $V_{++}(r)$ potentials in the harmonic approximation. Let's introduce relative coordinate variables $q_n = x_n - x_{n+1}$. In the new variables $\hat{H}_P = \sum_{n=1}^{N-1} P q_n$.

We split the total Hamiltonian (1) into a sum of two terms:

$$\hat{H} = \hat{H}_1 + \hat{H}_2, \tag{5}$$

where

$$\hat{H}_1 = \sum_{n=1}^{N-1} V^{(0)}_{s_n s_{n+1}} + \sum_{n=1}^{N} W_{s_n} \tag{6}$$

is a part of the Hamiltonian which does not contain q_n variables and

$$\hat{H}_2 = \frac{1}{2}\sum_{n=1}^{N-1} K_{s_n s_{n+1}} \left(q_n - a_{s_n s_{n+1}}\right)^2 + \sum_{n=1}^{N-1} P q_n \tag{7}$$

is a part of the Hamiltonian which depends on q_n. We note that both $\hat{H}_1$ and $\hat{H}_2$ depend on the spin variables. After some manipulations the Hamiltonian $\hat{H}_1$ yields the Ising-like form [22], and effects of degeneracy and the Hamiltonian $\hat{H}_2$ describe the pressure and temperature dependent corrections to the coefficients of the basic Ising model.

3. Partition function and effective Hamiltonian

The partition function completely determines the statistical properties of the model. By the definition

$$Z = \sum_{\langle s_1,\ldots,s_N\rangle} \iiint dq_1 \cdots dq_{N-1} g_{s_1} \cdots g_{s_N} \mathrm{e}^{-\beta E\left(q_1,\ldots,q_{N-1},s_1,\ldots,s_N\right)}, \tag{8}$$

where $E(q_1, \ldots, q_{N-1}, s_1, \ldots, s_N)$ is the energy, $\beta = 1/(k_B T)$ is the inverse temperature, k_B denotes the Boltzmann constant and the sum goes over all possible spin configurations $\langle s_1,\ldots,s_N\rangle$. Integration over phonon variables q_n gives the expression

$$Z = \sum_{\langle s_1,\ldots,s_N\rangle} g_{s_1} \cdots g_{s_N} \times \left[\prod_{n=1}^{N-1} \sqrt{\frac{2\pi}{\beta K_{s_n s_{n+1}}}} \exp\left(\frac{\beta P^2}{2K_{s_n s_{n+1}}} - \beta P a_{s_n s_{n+1}}\right)\right] \mathrm{e}^{-\beta E_1}. \tag{9}$$

Exponents in the partition function (9) are formed by terms of $\hat{H}_1$ only. We rewrite this part of the Hamiltonian in terms of pseudo-spin variables

$$\hat{H}_1 = E_0 - \sum_{n=1}^{N-1} J s_n s_{n+1} - \sum_{n=1}^{N-1} B \frac{s_n + s_{n+1}}{2} - W(s_1) - W(s_N), \tag{10}$$

where the following notations were introduced: the reference energy

$$E_0 = \frac{N-1}{4}\left(V^{(0)}_{--} + V^{(0)}_{++}\right) + \frac{N-1}{2} V^{(0)}_{+-} + N\frac{W_+ + W_-}{2},$$

the ferromagnetic constant $J = -\frac{1}{4}\left(V^{(0)}_{--} + V^{(0)}_{++}\right) + \frac{1}{2} V^{(0)}_{+-}$, the external field $B = \frac{1}{4}\left(V^{(0)}_{++} - V^{(0)}_{--}\right) - \frac{\Delta}{2}$, and the term acting on the edge spins $W(s_n) = -\frac{\Delta}{4} s_n$.

We express spin state degeneracies as follows:

$$g_{s_n} = \exp\left(\frac{1}{2}\left(\ln g_+ + \ln g_-\right) + \frac{1}{2}\left(\ln g_+ - \ln g_-\right) s_n\right). \tag{11}$$

The expression in the partition function (9) which we obtain during the integration over the phononic degrees of freedom we rewrite in the form

$$\sqrt{\frac{2\pi}{\beta K_{s_n s_{n+1}}}} \exp\left(\frac{\beta P^2}{2K_{s_n s_{n+1}}} - \beta P a_{s_n s_{n+1}}\right) = \exp\left(\varepsilon_P + \delta\varepsilon + (b_P + \delta b)(s_n + s_{n+1})/2 + (j_P + \delta j) s_n s_{n+1}\right). \tag{12}$$

where the energy term $\varepsilon_P = -\beta P a_\varepsilon + \frac{\beta P^2}{2K_\varepsilon}$, and the coefficients $j_P = -\beta P a_J + \frac{\beta P^2}{2K_J}$ and $b_P = -\beta P a_b + \frac{\beta P^2}{2K_B}$, with the characteristic distances expressed through the average distances at the equilibrium as follows

$$a_\varepsilon = \frac{1}{4}\left(a_{--} + a_{++}\right) + \frac{1}{2} a_{+-}, \quad a_J = \frac{1}{4}\left(a_{--} + a_{++}\right) - \frac{1}{2} a_{+-},$$

$$\text{and } a_B = \frac{1}{2}\left(a_{++} - a_{--}\right),$$

and characteristic elastic constants expressed through the elastic constants of the $V_{s_n s_{n+1}}(r)$ potentials as follows

$$\frac{1}{K_\varepsilon} = \frac{1}{4}\left(\frac{1}{K_{--}} + \frac{1}{K_{++}}\right) + \frac{1}{2}\frac{1}{K_{+-}},$$

$$\frac{1}{K_J} = \frac{1}{4}\left(\frac{1}{K_{--}} + \frac{1}{K_{++}}\right) - \frac{1}{2}\frac{1}{K_{+-}},$$

$$\frac{1}{K_B} = \frac{1}{2}\left(\frac{1}{K_{++}} - \frac{1}{K_{--}}\right).$$

The terms ε_P, j_P, and b_P take origin from the presence of pressure and vanish when $P \to 0$. The term $\delta\varepsilon = -\frac{1}{8}\ln\left(\frac{\beta^4}{(2\pi)^4} K^2_{+-} K_{--} K_{++}\right)$, and the coefficients,

$\delta j = \frac{1}{8}\ln\left(\frac{K_{+-}^2}{K_{--}K_{++}}\right)$ and $\delta b = \frac{1}{4}\ln\left(\frac{K_{--}}{K_{++}}\right)$ are manifestations of the elastic interaction.

Hence we have an expression for the partition function

$$Z = \sum_{\langle s_1,\ldots,s_N\rangle} \exp\left(\varepsilon + \sum_{n=1}^{N-1} v(s_n, s_{n+1}) + w(s_1) + w(s_N)\right), \quad (13)$$

where

$$w(s_n) = w\frac{s_n}{2}, \quad (14)$$

with the field acting on the edges $w = \frac{1}{2}\ln g - \frac{\beta\Delta}{2}$, and effective two-particle energy terms:

$$v(s_n, s_{n+1}) = j s_n s_{n+1} + b(s_n + s_{n+1})/2, \quad (15)$$

and

$$\varepsilon = \varepsilon_P - \beta E_0 + \frac{N}{2}\ln\left(g_+ g_-\right) + (N-1)\delta\varepsilon, \quad (16a)$$

$$j = j_P + \beta J + \delta j, \quad (16b)$$

$$b = b_P + \beta B + \frac{1}{2}\ln g + \delta b. \quad (16c)$$

We make notation $g = \frac{g_+}{g_-}$.

The partition function (13) can be expressed as the partition function of the Ising-like model with the effective Hamiltonian:

$$\hat{H}_{\text{eff}} = E_{0,\text{eff}} - \sum_{n=1}^{N-1} J_{\text{eff}} \hat{s}_n \hat{s}_{n+1} - \sum_{n=2}^{N-1} B_{\text{eff}} \hat{s}_n + \\ + \frac{B_{\text{bound}} + B_{\text{eff}}}{2}(\hat{s}_1 + \hat{s}_N), \quad (17)$$

where the reference energy $E_{0,\text{eff}} = E_0 - \frac{Nk_BT}{2}\ln g_+ g_- - (N-1)\delta\varepsilon k_BT - (N-1)Pa_\varepsilon + (N-1)\frac{P^2}{2K_\varepsilon}$, the ferromagnetic interaction constant $J_{\text{eff}} = J + \delta j k_BT + Pa_J - \frac{P^2}{2K_J}$, the field acting on the bulk $B_{\text{eff}} = B + \frac{k_BT}{2}\ln g + \delta b k_BT + Pa_b - \frac{P^2}{2K_B}$, and field acting on the boundaries $B_{\text{bound}} = -\frac{\Delta}{2} + \frac{k_BT}{2}\ln g$. The effective Hamiltonian coincides with the Hamiltonian of the Ising model in which the reference energy, effective magnetic field [39, 40], and ferromagnetic interaction constant are functions of temperature and pressure. This dependence on temperature roots from the taking into account pseudo-states degeneracy and phononic interactions. In the limit $P \to 0$ and $K_{++} = K_{+-} = K_{--}$, phonon degrees of freedom are decoupled from the spin degrees of freedom, thus the effective ferromagnetic interaction constant $J_{\text{eff}} \to J$ and the effective external field $B_{\text{eff}} \to B$.

4. Transfer-matrix formalism

The thermodynamic properties of the system are completely described by the partition function. Here, we use the transfer matrix formalism [22, 41, 42] to calculate the partition function. We rewrite the partition function (13) in the following form:

$$Z = \mathrm{e}^{\varepsilon}\mathrm{Tr}\hat{T}^{N-1}\hat{R}, \quad (18)$$

where the transfer matrix is

$$\hat{T} = \mathrm{e}^{v(s_n, s_{n+1})} = \begin{pmatrix} \mathrm{e}^{j+b} & \mathrm{e}^{-j} \\ \mathrm{e}^{-j} & \mathrm{e}^{j-b} \end{pmatrix}, \quad (19)$$

and the matrix $\hat{R}$ is accounting effects of the field acting on the surface spins

$$\hat{R} = \mathrm{e}^{w(s_N)+w(s_1)} = \begin{pmatrix} \mathrm{e}^{w} & 1 \\ 1 & \mathrm{e}^{-w} \end{pmatrix}. \quad (20)$$

For calculating $\mathrm{Tr}\hat{T}^{N-1}\hat{R}$ we change the basis to the eigenbasis of the transfer matrix:

$$Z = \mathrm{e}^{\varepsilon}\mathrm{Tr}\hat{U}\hat{U}^{-1}\hat{T}^{N-1}\hat{U}\hat{U}^{-1}\hat{R}, \quad (21)$$

where

$$\hat{U} = \begin{pmatrix} \cos\phi & \sin\phi \\ -\sin\phi & \cos\phi \end{pmatrix}, \quad (22)$$

and the angle of rotation ϕ is given by a solution of the equation

$$\cot 2\phi = \mathrm{e}^{2j}\sinh b. \quad (23)$$

The eigenvalues of the transfer matrix $\hat{T}$ are

$$\lambda_\pm = \left(\mathrm{e}^{j}\cosh b \pm \sqrt{\mathrm{e}^{2j}\sinh^2 b + \mathrm{e}^{-2j}}\right). \quad (24)$$

Therefore we obtain the partition function for the system of N particles

$$Z = \mathrm{e}^{\varepsilon}\left(c_+\lambda_+^{N-1} + c_-\lambda_-^{N-1}\right), \quad (25)$$

where the coefficients are

$$c_+ = \cosh w + \frac{\mathrm{e}^{-2j} + \sinh b \sinh w}{\sqrt{\sinh^2 b + \mathrm{e}^{-4j}}}, \quad (26a)$$

$$c_- = \cosh w - \frac{\mathrm{e}^{-2j} + \sinh b \sinh w}{\sqrt{\sinh^2 b + \mathrm{e}^{-4j}}}. \quad (26b)$$

Until now all calculation were exact and the partition function (25) contains all finite N effects. The free energy density is given by the following expression:

$$f = -\frac{1}{N\beta}\ln Z. \tag{27}$$

In the thermodynamic limit, we obtain

$$f = -\lim_{N\to\infty}\frac{1}{\beta N}\ln Z = -\frac{\varepsilon}{N\beta} - \frac{1}{\beta}\ln\lambda_+. \tag{28}$$

Average magnetization per quasi-spin is $m = \langle s\rangle = \frac{1}{N}\frac{\partial \ln Z}{\partial b}$. The magnetization per spin in the thermodynamic limit $\langle s\rangle$ at nonzero temperature T, pressure P, and external field B are easily evaluated:

$$m = \frac{\sinh b}{\sqrt{\sinh^2 b + \mathrm{e}^{-4j}}}. \tag{29}$$

Average magnetization given by the Eq. (32) has the same form as one of the Ising model but in our model the dependence of b and j from the temperature and pressure is different from one of the Ising model. The fraction of molecules in the HS state is given by the occupation number $n_{HS} = \frac{1+\langle s\rangle}{2}$ and the fraction of the molecules in the LS state is $n_{LS} = \frac{1-\langle s\rangle}{2}$. Results for zero pressure, symmetric degeneracies case $g_+ = g_-$ and without phononic part repeat well-known behavior of conventional Ising model.

In Fig. 2 the dependencies of the fraction molecules in the HS state on the temperature for various values of pressure are plotted. The parameters of the model are chosen to be following: $a_B / a_\varepsilon = 0.104$, $a_J / a_\varepsilon = 0.0104$, $K_\varepsilon / K_B = 1.28$, and $K_\varepsilon / K_J = 0.57$ with $K_J a_J^2 = 72J$. The thermal behavior of the molecular fraction $n_{HS}(T)$ characterizes the nature of transitions that may be abrupt or gradual, depending on the choice of the values of T_{eq} and T_{cros}. Under small pressure, the cooperativity decreases and the transition becomes less abrupt at higher temperatures.

5. Average volume and the correlation function

Let's calculate average effective volume of the finite molecular chain

$$L = \sum_{n=1}^{N-1}\langle x_{n+1} - x_n\rangle = \sum_{n=1}^{N-1}\langle q_n\rangle. \tag{30}$$

By the definition, the average distance between the nearest molecules is

$$\langle q_n\rangle = \frac{1}{Z}\sum_{\langle s_1,\ldots,s_N\rangle}\iiint dq_1\cdots dq_{N-1}q_n g_{s_1}\cdots g_{s_N}\mathrm{e}^{-\beta E}. \tag{31}$$

Integrating over the phonon degrees of freedom we get

$$\langle q_n\rangle = \frac{\sum\limits_{\langle s_1,\ldots,s_N\rangle}\left(a_{s_n s_{n+1}} - \dfrac{P}{K_{s_n s_{n+1}}}\right)\mathrm{e}^{-\beta H_{\mathrm{eff}}}}{\sum\limits_{\langle s_1,\ldots,s_N\rangle}\mathrm{e}^{-\beta H_{\mathrm{eff}}}}. \tag{32}$$

Suchwise, the effective volume of system (length of molecular chain) is $L = \sum_{n=1}^{N-1}\langle a_{s_n s_{n+1}} - \frac{P}{K_{s_n s_{n+1}}}\rangle$. We rewrite later expression as follows:

$$L = \sum_{n=1}^{N-1}\left(a_\varepsilon - \frac{P}{K_\varepsilon} + (a_J - \frac{P}{K_J})\langle s_n s_{n+1}\rangle + \right.$$
$$\left. + \left(\frac{a_B}{2} - \frac{P}{2K_B}\right)\langle s_n + s_{n+1}\rangle\right). \tag{33}$$

Thus, the effective volume of the system is connected with the average magnetization and the correlation function. The local magnetization may be calculated directly [22]

$$\langle \hat{s}_n\rangle = m + \frac{C_{+-}\mathrm{e}^{-\frac{n-1}{\xi}} + C_{-+}\mathrm{e}^{-\frac{N-n}{\xi}}}{c_+ + c_-\mathrm{e}^{-\frac{N-1}{\xi}}}, \tag{34}$$

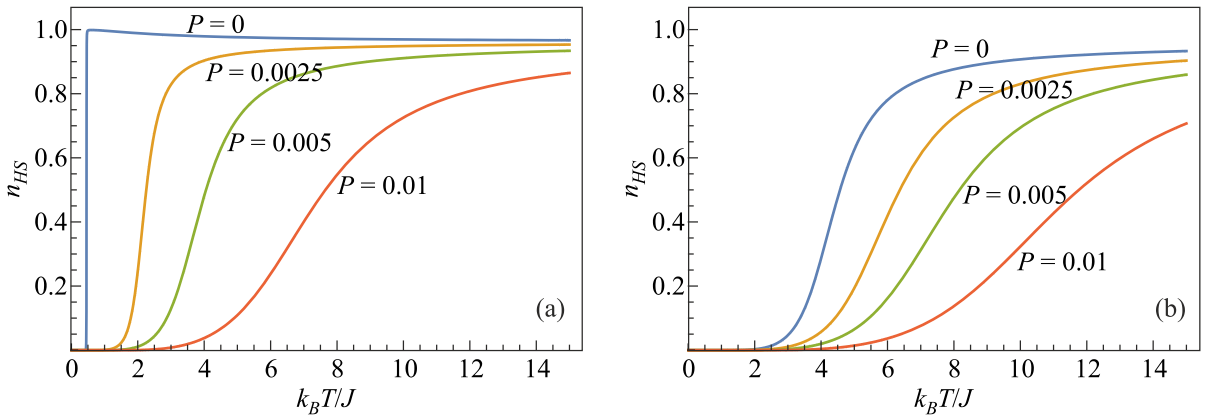

Fig. 2. Average occupation number n_{HS} as a function of temperature for $T_{\mathrm{eq}} < T_{\mathrm{cros}}$ (a) and $T_{\mathrm{eq}} > T_{\mathrm{cros}}$ (b) and various values of pressure $P = 0$, 0.0025, 0.005, 0.01, and $\frac{1}{2}\ln g + \delta b = 0.5$ and $\delta j = 0.35$.

where coefficients

$$C_{-+} = C_{+-} = (m^2 - 1)(-\sinh w + \mathrm{e}^{2j}\sinh b), \qquad (35)$$

and the correlation length $\xi = -\ln(\lambda_-/\lambda_+)$. It is easy to see that since $\lambda_- < \lambda_+$, $\xi > 0$. The average magnetization is

$$\langle \hat{s} \rangle = m + \frac{C_{+-} + C_{-+}}{N\left(1 - \mathrm{e}^{-\frac{N}{\xi}}\right)\left(c_+ + c_- \mathrm{e}^{-\frac{N-1}{\xi}}\right)}. \qquad (36)$$

In the thermodynamic limit, we get classic Ising model magnetization $\langle \hat{s} \rangle = m$. We note that only average over all spins magnetization coincides with the classic Ising model result, while the average of the individual spin is distinct from the classic result due to the system boundary. We see boundary effects do not vanish even in the thermodynamic limit.

The local correlation function $G_n(r)$ is [22]

$$G_n(r) = \langle \hat{s}_n \hat{s}_{n+r} \rangle = m^2 + (1-m^2)\frac{c_+ \mathrm{e}^{-\frac{r}{\xi}} + c_- \mathrm{e}^{-\frac{N-r-1}{\xi}}}{c_+ + c_- \mathrm{e}^{-\frac{N-1}{\xi}}} +$$

$$+ mC_{+-}\frac{\mathrm{e}^{-\frac{n-1}{\xi}} - \mathrm{e}^{-\frac{n-1+r}{\xi}} + \mathrm{e}^{-\frac{N-n-r}{\xi}} - \mathrm{e}^{-\frac{N-n}{\xi}}}{c_+ + c_- \mathrm{e}^{-\frac{N-1}{\xi}}}. \qquad (37)$$

In the thermodynamic limit, we get the correlation function

$$G(r) = \frac{1}{N}\sum_{n=1}^{N-r-1} \langle \hat{s}_n \hat{s}_{n+r} \rangle = m^2 + (1-m^2)\mathrm{e}^{-\frac{r}{\xi}}. \qquad (38)$$

The average magnetization given by the Eq. (37) and the correlation function given by the Eq. (40) are exact. We see the average correlation function matches with the classic Ising model result [4] in the thermodynamic limit. Local correlation function [see Eq. (40)] has information about the edges of the system even in the thermodynamic limit.

Finally, we get the length of chain

$$L = (N-1)\left[a_\varepsilon - \frac{P}{K_\varepsilon} + \left(a_B - \frac{P}{K_B}\right)m + \left(a_J - \frac{P}{K_J}\right)G(1)\right] +$$

$$+\left(a_B - \frac{P}{K_B}\right)\frac{C_{+-} + C_{-+}}{c_+ + c_- \mathrm{e}^{-\frac{N-1}{\xi}}}\left[\frac{1}{1-\mathrm{e}^{-\frac{N}{\xi}}} - \frac{1}{2}(1 + \mathrm{e}^{-\frac{N-1}{\xi}})\right] +$$

$$+\left(a_J - \frac{P}{K_J}\right)m\frac{C_{+-}(1-\mathrm{e}^{-\frac{1}{\xi}})}{c_+ + c_- \mathrm{e}^{-\frac{N-1}{\xi}}}\left[\frac{1}{1-\mathrm{e}^{-\frac{N-1}{\xi}}} + \frac{\mathrm{e}^{-\frac{N-1}{\xi}}}{1-\mathrm{e}^{\frac{N-1}{\xi}}}\right]. \qquad (39)$$

Expression (39) is exact and, in the thermodynamic limit, defines average density of the molecular chain

$$\rho^{-1} = L/N \to a_\varepsilon - \frac{P}{K_\varepsilon} + \left(a_B - \frac{P}{K_B}\right)m + \left(a_J - \frac{P}{K_J}\right)G(1).$$

The only approximation we made is the harmonic approximation of the interparticle potential. This approximation should be valid when the displacement of particles from the equilibrium distances is small. Applied external pressure clearly reduces the distances between the particles and at some point harmonic approximation loses its validity. Equation (39) gives us some understanding of the harmonic approximation limits. The volume of the system should be positive, therefore we external pressure should satisfy the following condition $P \ll P_\varepsilon = a_\varepsilon K_\varepsilon$.

6. Specific heat capacity and susceptibility

The specific heat capacity is one of the most important thermodynamic characteristic of the system which can be easily measured experimentally. We consider a system under a constant pressure, and therefore the volume of the system changes. The internal energy per particle is $\langle E \rangle = -\frac{\partial}{\partial \beta}\ln Z$,

$$\langle E \rangle = E_0 + \frac{1}{2}Nk_BT - \sum_{n=1}^{N-1}\left(J + a_J P - \frac{P^2}{2K_J}\right)\langle s_n s_{n+1} \rangle -$$

$$-\sum_{n=1}^{N}\left(B + a_B P - \frac{P^2}{2K_B}\right)\langle s_n \rangle. \qquad (40)$$

And the heat capacity per particle $c_P = \frac{1}{N}\frac{\partial \langle E \rangle}{\partial T}$ in the thermodynamic limit can be written in the following way:

$$c_P = \frac{1}{2}k_B - \left(B + a_B P - \frac{P^2}{2K_B}\right)\frac{\partial m}{\partial T} -$$

$$-\left(J + a_J P - \frac{P^2}{2K_J}\right)\frac{\partial}{\partial T}G(1). \qquad (41)$$

Specific heat capacities per particle for small pressures are given in Fig. 3. Parameters of the model in Figs. 3 and 4 are the same as in Fig. 2. One-dimensional systems demonstrate two-peak specific heat capacity thermal behavior on experiments [13]. Our model captures this phenomenon at small pressure in the abrupt crossover regime. Main peak is associated with the Schottky anomaly. This result may be expected as we demonstrated the exact mapping onto the Ising-like system with the Hamiltonian (17). Such behavior appears as a result of the initial assumption about the nature of iron(II) materials that only two lowest single-molecule levels (denoted LS and HS) are relevant for the description of the system. With the increase of pressure the main peak of specific heat capacity become broader and shifts to higher temperatures. Such behavior quickly disappears with pressure increase.

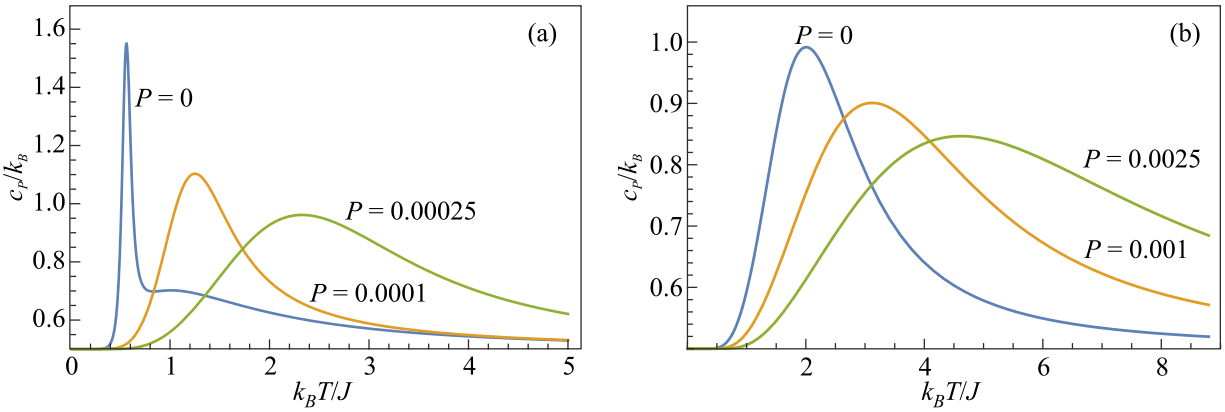

Fig. 3. Specific heat capacity per particle c_P as a function of temperature for various pressure (a) $T_{eq} = 0.3T_{cros}$, (b) $T_{eq} = 3T_{cros}$. With the pressure increase peak of the specific heat capacity shifts to higher temperatures.

The susceptibility $\chi = 2\dfrac{\partial n_{HS}}{\partial B}$, is

$$\chi = \frac{1}{k_B T}\frac{\cosh(b)\mathrm{e}^{-4j}}{\left(\sinh^2 b + \mathrm{e}^{-4j}\right)^{\frac{3}{2}}}. \qquad (42)$$

The susceptibility as a function of k_BT/J under various pressure is shown in Fig. 4. Similarly to the specific heat capacity, with the pressure increase the peak of the susceptibility shifts to higher temperatures and becomes broader.

7. Spin crossover under the pressure

In our previous paper [22], we investigated regimes of gradual and abrupt crossover under zero pressure $P = 0$. We introduced two characteristic values of the system, namely the equilibrium T_{eq} and the crossover temperature T_{cros}. We demonstrated that if $T_{eq} < T_{cros}$ the crossover is abrupt and some thermal quantities resemble ones for the phase transition, and if $T_{eq} < 0$ or $T_{eq} > T_{cros}$ the crossover is gradual. Here our goal is to explore what changes crossover undergo in the case $P \neq 0$. At zero temperature system always stays in ordered phase which is defined by the sign of the effective field:

$$n_{HS}(T \to 0) = \frac{1}{2}\left[1 + \mathrm{sign}\left(B + a_B P - \frac{P^2}{2K_B}\right)\right]. \qquad (43)$$

Usually, in Fe (II) compounds $B > 0$ and LS is lower than HS state under zero pressure, thus $n_{HS}(T \to 0) = 0$. Nevertheless for large pressure $B + a_B P - \dfrac{P^2}{2K_B} < 0$ and therefore crossover starts from $n_{HS}(T \to 0) = 1$. At the same time at high temperatures occupation numbers are

$$n_{HS}(T \to \infty) = \frac{1}{2} + \frac{1}{2}\frac{\sinh\left(\frac{1}{2}\ln g + \delta b\right)}{\sqrt{\sinh^2\left(\frac{1}{2}\ln g + \delta b\right) + \mathrm{e}^{-4\delta j}}}. \qquad (44)$$

We introduce the equilibrium temperature T_{eq} as a temperature when pseudo-spin states have equal occupations $n_{HS} = 1/2$. Often the equilibrium temperature is denoted as $T_{1/2}$. This happens when the effective field vanishes,

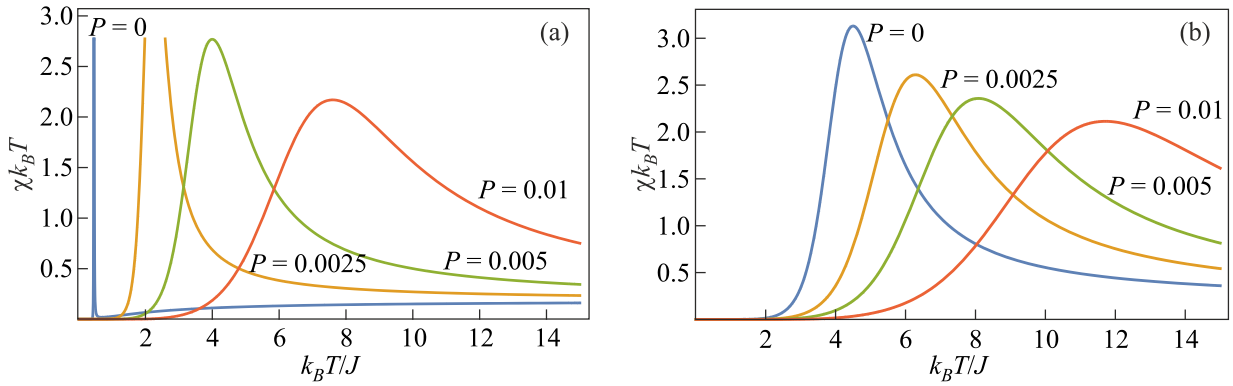

Fig. 4. Susceptibility χ as a function of temperature for various pressure (a) $T_{eq} = 0.3T_{cros}$, (b) $T_{eq} = 3T_{cros}$. With the pressure increase peak of the susceptibility shifts to higher temperatures.

i.e., $b = 0$. In doing so, one gets the following expression for the equilibrium temperature $T_{\rm eq}$ as a function of the pressure:

$$T_{\rm eq}(P) = -\frac{B - Pa_b + \dfrac{P^2}{2K_B}}{k_B\left(\dfrac{1}{2}\ln g + \delta b\right)}. \tag{45}$$

We note that for certain values of the external field B, pressure P and pseudo-spin degeneracies g the equilibrium temperature $T_{\rm eq}$ can be negative what means that for given field and degeneracies there is no such temperature that pseudo-spin states would have equal occupations.

Let's find a temperature T_0 for which the occupation number is maximal. This temperature should be a solution of the equation

$$\left.\frac{\partial n_{HS}}{\partial T}\right|_{T=T_0} = 0. \tag{46}$$

Therefore

$$T_0 = \frac{T_{\rm eq}(P)}{1 - \dfrac{1}{\dfrac{1}{2}\ln g + \delta b}\operatorname{arctanh}\left(\dfrac{k_B T_{\rm eq}(P)}{2\left(J + Pa_J - \dfrac{P^2}{2K_J}\right)}\left(\dfrac{1}{2}\ln g + \delta b\right)\right)}. \tag{47}$$

We call the maximal equilibrium temperature $T_{\rm eq}$ at which Eq. (49) has finite solutions for the T_0 as the crossover temperature. The derivative $\partial n_{HS}/\partial T$ is always positive and the occupation number n_{HS} is a monotonous function of temperature when $T_{\rm eq} < T_{\rm cros}$. Thus we get the crossover temperature

$$T_{\rm cros}(P) = \frac{2\left(J + Pa_J - \dfrac{P^2}{2K_J}\right)}{k_B}\frac{\tanh\left(\dfrac{1}{2}\ln g + \delta b\right)}{\dfrac{1}{2}\ln g + \delta b}. \tag{48}$$

The crossover temperature $T_{\rm cros}(P) > T_{\rm cros}(0)$ when the pressure $P < P_J = 2K_J a_J$, and $T_{\rm cros}(P) < T_{\rm cros}(0)$ when $P > P_J$. Therefore we shall observe abrupt crossover when $T_{\rm cros}(P) > 0$ and $T_{\rm eq}(P) < T_{\rm cros}(P)$, and gradual crossover otherwise.

The resulting phase diagram for the spin crossover is presented in Fig. 5. In left and central panels (a), (b) occupation number is depicted for temperature and pressure values close to zero. A spin crossover phase diagram, where the HS fraction is indicated by color, is shown in a wide range of temperature and pressure variations in Fig. 5(c). The diagram shows regions of the HS paramagnetic phases under high pressure and the LS diamagnetic phase at relatively low temperature and pressure. We observe two regions with abrupt HS–LS transitions: the region near $P = 0$ and $P = P_J$. For $T_{\rm eq}(0) > T_{\rm cros}(0)$, it can be seen that no sharp discontinuous changes in n_{HS}, therefore in structural or optical properties, should be expected to occur across this spin crossover. As the pressure increases, the width of the SCO region is broadened, the sharp spin transition becomes a smoother and broader SCO. Evidently, system undergoes a sharp HS–LS transition with a very narrow SCO region at low temperature when $T_{\rm eq} < T_{\rm cros}$.

8. Summary and conclusions

This paper aimed to give a thorough discussion of the thermodynamic properties of the one-dimensional spin-crossover systems being a subject of constant pressure. We start with the exact microscopic Hamiltonian which consists of sum of the pair intermolecular potentials. In the harmonic approximation, we demonstrate exact mapping to the Ising-like Hamiltonian with temperature dependent effective parameters of the model, namely the reference energy, ferromagnetic constant, and magnetic field. For this purpose, the transfer-matrix method was transformed to form that addresses free-boundary case. The elaborated rigorous procedure has enabled us to derive exact results for the basic thermodynamic quantities and pair correlation function. In the framework of this approach we show that the degeneracy of the levels, elastic interaction and pres-

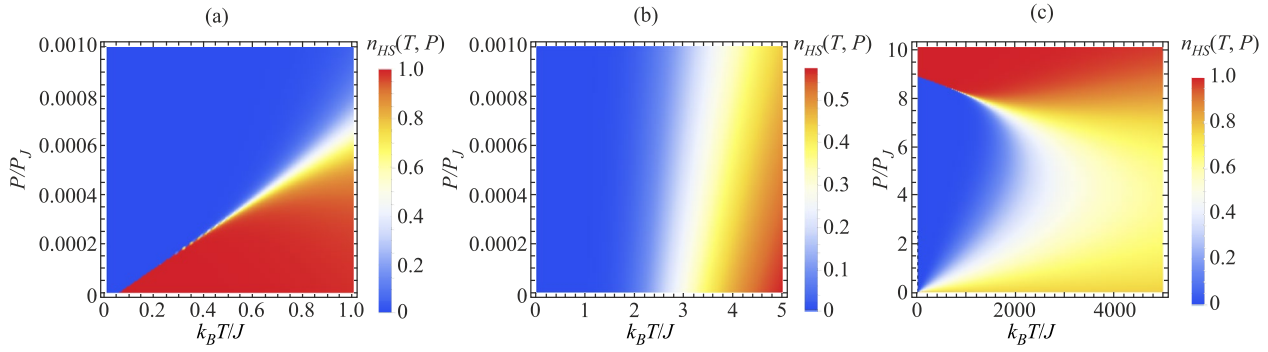

Fig. 5. (Color online) Phase diagram of the average occupation number $n_{HS}(T,P)$. (a) small T, P region for $T_{\rm eq}(P=0) < T_{\rm cros}$, (b) small T, P region for $T_{\rm eq}(P=0) > T_{\rm cros}$, (c) large scale T, P dependence. Colors in the vertical column on the right represent the fraction of high-spin molecules.

sure renormalize the parameters of the effective Ising model. We analyze regimes of the HS–LS crossover and identify regions of parameters where the crossover abrupt or gradual and show how pressure effects on the location and size of the transition. In the next works, we are planning to extend our results to higher dimensions and experimental situations.

1. C. M. Jureschi, J. Linares, A. Rotaru, M. H. Ritti, M. Parlier, M. M. Dîrtu, M. Wolff, and Y. Garcia, *Sensors* **15**, 2388 (2015).
2. Iu. Gudyma, C. Enachescu, and A. Maksymov, *Kinetics of Nonequilibrium Transition in Spin-crossover Compounds*, in: *Nanocomposites, Nanophotonics, Nanobiotechnology, and Applications*, Springer (2015), p. 375.
3. *Spin-crossover Materials: Properties and Applications*, M. A. Halcrow (ed.), John Wiley & Sons (2013).
4. P. Gütlich, A. Hauser, and H. Spiering, *Angewandte Chemie International Edition in English* **33**, 2024 (1994).
5. E. Coronado, *Nature Rev. Mater.* **5**, 87 (2020).
6. P. Gütlich, H. A. Goodwin, and Y. Garcia, *Spin-crossover in Transition Metal Compounds I*, Springer Science & Business Media (2004), Vol. 1.
7. A. Bousseksou, G. Molnár, L. Salmon, and W. Nicolazzi, *Chem. Soc. Rev.* **40**, 3313 (2011).
8. Y. Garcia, V. Ksenofontov, G. Levchenko, and P. Gütlich, *J. Mater. Chem.* **10**, 2274 (2000).
9. A. Sugahara, H. Kamebuchi, A. Okazawa, M. Enomoto, and N. Kojima, *Inorganics* **5**, 50 (2017).
10. K. Nebbali, C. D. Mekuimemba, C. Charles, S. Yefsah, G. Chastanet, A. J. Mota, E. Colacio, and S. Triki, *Inorganic Chem.* **57**, 12338 (2018).
11. Ju. A Wolny, T. Hochdörffer, S. Sadashivaiah, H. Auerbach, K. Jenni, L. Scherthan, Ai-Min Li, C. von Malotki, H.-C. Wille, and E. Rentschler, *J. Phys.: Condens. Matter* **33**, 034004 (2020).
12. M. Weselski, M. Książek, J. Kusz, A. Białońska, D. Paliwoda, M. Hanfland, F. Rudolf, Z. Ciunik, and R. Bronisz, *Eur. J. Inorganic Chem.* **2017**, 1171 (2017).
13. M. M. Dîrtu, F. Schmit, A. D. Naik, I. Rusu, A. Rotaru, S. Rackwitz, J. A. Wolny, V. Schünemann, L. Spinu, and Y. Garcia, *Chem. A European J.* **21**, 5843 (2015).
14. D. Maskowicz, M. Sawczak, A. C. Ghosh, K. Grochowska, R. Jendrzejewski, A. Rotaru, Y. Garcia, and G. Śliwiński, *Appl. Surface Science* **541**, 148419 (2021).
15. S. Ostrovsky, A. Palii, S. Decurtins, S.-X. Liu, and S. Klokishner, *J. Phys. Chem. C* **122**, 22150 (2018).
16. G. Levchenko, A. Khristov, V. Kuznetsova, and V. Shelest, *J. Phys. Chem. Solids* **75**, 966 (2014).
17. R. Traiche, M. Sy, and K. Boukheddaden, *J. Phys. Chem. C* **122**, 4083 (2018).
18. W. Nicolazzi, J. Pavlik, S. Bedoui, G. Molnár, and A. Bousseksou, *Europ. Phys. J. Special Top.* **222**, 1137 (2013).
19. T. D. Oke, F. Hontinfinde, and K. Boukheddaden, *Appl. Phys. A* **120**, 309 (2015).
20. O. Rojas, J. Strečka, M. L. Lyra, and S. M. de Souza, *Phys. Rev. E* **99**, 042117 (2019).
21. T. Hutak, T. Krokhmalskii, O. Rojas, S. Martins de Souza, and O. Derzhko, *Phys. Lett. A* **387**, 127020 (2021).
22. A. Gudyma and Iu. Gudyma, *J. Appl. Phys.* **129**, 123905 (2021).
23. V. A. Zagrebnov and B. K. Fedyanin, *Theor. Mathem. Phys.* **10**, 84 (1972).
24. S. R. Salinas, *J. Phys. A* **6**, 1527 (1973).
25. V. B. Henriques and S. R. Salinas, *J. Phys. C* **20**, 2415 (1987).
26. A. H. Marshall, B. Chakraborty, and S. Nagel, *Europhys. Lett.* **74**, 699 (2006).
27. T. Balcerzak, K. Szałowski, and M. Jaščur, *J. Magn. Magn. Mater.* **507**, 166825 (2020).
28. T. Nakada, T. Mori, S. Miyashita, M. Nishino, S. Todo, W. Nicolazzi, and P. A. Rikvold, *Phys. Rev. B* **85**, 054408 (2012).
29. H.-Z. Ye, C. Sun, and H. Jiang, *Phys. Chem. Chem. Phys.* **17**, 6801 (2015).
30. H. Banerjee, M. Kumar, and T. Saha-Dasgupta, *Phys. Rev. B* **90**, 174433 (2014).
31. A. M. Apetrei, K. Boukheddaden, and A. Stancu, *Phys. Rev. B* **87**, 014302 (2013).
32. A. B. Gaspar, G. Molnár, A. Rotaru, and H. J. Shepherd, *Comptes Rendus Chimie* **21**, 1095 (2018).
33. Iu. Gudyma, V. Ivashko, and J. Linares, *J. Appl. Phys.* **116**, 173509 (2014).
34. Iu. V. Gudyma, A. I. Maksymov, and V. V. Ivashko, *Nanoscale Res. Lett.* **9**, 1 (2014).
35. Iu. V. Gudyma and V. V. Ivashko, *Nanoscale Res. Lett.* **11**, 196 (2016).
36. W. Nicolazzi, S. Pillet, and C. Lecomte, *Phys. Rev. B* 78, 174401 (2008).
37. V. Legrand, S. Pillet, C. Carbonera, M. Souhassou, J.-F. Létard, P. Guionneau, and C. Lecomte, *European J. Inorganic Chem.* **36**, 5693 (2007).
38. J. Jung, F. Bruchhäuser, R. Feile, H. Spiering, and P. Gütlich, *Z. Phys. B* **100**, 517 (1996).
39. A. Bousseksou, J. Nasser, J. Linares, K. Boukheddaden, and F. Varret, *J. Phys. I* **2**, 1381 (1992).
40. K. Boukheddaden, J. Linares, H. Spiering, and F. Varret, *The European Physical Journal B-Condensed Matter and Complex Systems* **15**, 317 (2000).
41. J. Nasser, K. Boukheddaden, and J. Linares, *European Phys. J. B* **39**, 219 (2004).
42. K. Boukheddaden, S. Miyashita, and M. Nishino, *Phys. Rev. B* 75, 094112 (2007).
43. S. Bellucci and V. Ohanyan, *European Phys. J. B* **86**, 446 (2013).

Вплив стискування на молекулярні спін-кросоверні ланцюжки

A. Gudyma, Iu. Gudyma

Досліджено термодинамічні властивості одновимірного спін-кросоверного молекулярного ланцюжка, що знаходиться під постійним зовнішнім тиском. Як теоретична основа використовується ефективна вироджена стислива модель Ізінга. З використанням формалізму трансфер-матриці отримано аналітичні результати щодо кросовера від низькоспінових до високоспінових станів. Отримано точні вирази для частки молекул у високоспіновому стані, кореляційної функції та теплоємності. Проведено аналіз області параметрів, у якій відбувається спіновий кросовер. Показано, як тиск змінює положення кросовера.

Ключові слова: спін-кросовер, молекулярний ланцюжок, модель Ізінга, намагніченість, фонони.